Bull. Mater. Sci., Vol. 35, No. 6, November 2012, pp. 1019–1029. © Indian Academy of Sciences.

Artificial neural networks for prediction of percentage of water absorption of geopolymers produced by waste ashes

ALI NAZARI
Department of Materials Science and Engineering, Saveh Branch, Islamic Azad University, Saveh, Iran

MS received 18 July 2011; revised 14 February 2012

Abstract. **In the present work, percentage of water absorption of geopolymers made from seeded fly ash and rice husk bark ash has been predicted by artificial neural networks. Different specimens, made from a mixture of fly ash and rice husk bark ash in fine and coarse form together with alkali activator made of water glass and NaOH solution, were subjected to permeability tests at 7 and 28 days of curing. The curing regime was different: one set cured at room temperature until reaching to 7 and 28 days and the other sets were oven cured for 36 h at a range of 40–90 °C and then cured at room temperature for 7 and 28 days. To build the model, training and testing using experimental results from 120 specimens were conducted. According to these input parameters, in the neural networks model, the percentage of water absorption of each specimen was predicted. The training and testing results in the neural networks model have shown a strong potential for predicting the percentage of water absorption of the geopolymer specimens.**

Keywords. **Geopolymer; fly ash; rice husk bark ash; percentage of water absorption; artificial neural networks.**

1. Introduction

Most building materials have typical porous structure and composed of solid matrix and pores with moisture in them. Permeability of building materials is defined as the movement of liquid and/or gas through a mass of concrete under a constant pressure gradient. It is an inherent property of construction materials that chiefly depends upon the geometric arrangement and characteristics of the constituent materials. The moisture transfer in building materials connects the durability, inside humidity level and energy performance of the building (Fanhong and Maoyu 2008; Tariku *et al* 2010). Moreover, the moisture transferring in building materials can cause metal corrosion, structure deterioration and improper performance of building insulations.

Inorganic polymers, also known as geopolymers, are X-ray amorphous materials, usually aluminosilicates, composed of a network of randomly arranged silicate and aluminate tetrahedra in conjunction with charge balancing alkali metal cations (Barbosa *et al* 2000). They generally have high compressive strengths in comparison with concrete specimens together with high water resistivity. Aluminosilicate geopolymers are conventionally synthesized at approximately ambient temperature by reaction of a solid aluminosilicate source, e.g. dehydroxylated kaolin clay (metakaolinite) with an alkali silicate solution under highly alkaline conditions (Davidovits 2008). Industrial wastes such as fly ash or blast furnace slag have also been proposed as solid reactants, especially for low-energy cement applications (Davidovits 2008), but the resulting products are more properly described as alkali-activated cements. The main properties of geopolymers are: quick compressive strength development, low permeability, resistance to acid attack, good resistance to freeze-thaw cycles, and tendency to drastically decrease the mobility of most heavy metal ions contained within the geopolymeric structure (van Jaarsveld *et al* 1997). Such properties make them interesting structural products, such as concrete replacements in various environments, and immobilization systems for heavy metal containment (Álvarez-Ayuso *et al* 2008).

The properties of inorganic polymers depend on both the ratio of Si/Al and the types of utilized raw material. Fly ash (FA) is recently used as a source material to produce geopolymer because of its suitable chemical composition along with favourable size and shape. Fly ash is a byproduct of coal-fired electric power stations. Literature survey specifies that fly ash is primarily composed of SiO_2, Al_2O_3 and Fe_2O_3. Since the quality of fly ash depends on the type and quality of coal along with the performance of the power plant, difficulties sometimes remain to control its chemical composition. In order to achieve a suitable chemical composition to produce geopolymers, the preferred method is to blend fly ash with another high silica source (Wongpa *et al* 2010).

Rice husk–bark ash (RH–BA) is a solid waste generated by biomass power plants using rice husk and eucalyptus bark as fuel. The power plant company providing RH–BA for this research reported that about 450 tons/day of RH–BA are produced and discarded. The major chemical constituent

*Author for correspondence (alinazari84@aut.ac.ir)

of RH–BA is SiO_2 (about 75%) (Sata *et al* 2007). Therefore, blending FA and RH–BA can adjust the ratio of Si/Al as required.

Over the last two decades, a different modelling method based on neural networks (ANNs) has become popular and used by many researchers for a wide range of engineering applications. ANNs are a family of massively parallel architectures that solve difficult problems via the cooperation of highly interconnected but simple computing elements (or artificial neurons). Basically, the processing elements of a neural network are analogous to the neurons in the brain, which consist of many simple computational elements arranged in several layers (Pala *et al* 2005). Some models have been recently proposed to predict Charpy impact behaviour using neural network (Cottrell *et al* 2007; Pak *et al* 2009); these models are at their infancy and need to be extended.

As per our knowledge, there are no results reported on utilizing a mixture of FA and RH–BA with seeded distribution of particles to produce geopolymers. In addition, since the concept of geopolymers is completely new and there are only a few works on their properties, application of computer programs like neural networks to predict their properties is rarely reported. The aim of this study is to investigate the percentage of water absorption of geopolymers produced from seeded FA and RH–BA mixture experimentally and presenting suitable model based on artificial neural networks (ANNs) to predict their percentage of water absorption. Both FA and RH–BA with two different particle size distributions have been mixed with different amounts to produce four classes of geopolymers. Percentage of water absorption of the produced specimens has been investigated after specific times of curing. Totally 120 data of permeability tests in different conditions were collected, trained and tested by means of ANNs. The obtained results have been compared by experimental ones to evaluate the software power for predicting the percentage of water absorption of the geopolymer specimens.

2. Experimental

The cementitious materials used in this work were FA and RH–BA. Their chemical composition has been illustrated in table 1 (Nazari and Riahi 2012). In addition, figure 1 shows SEM micrograph of the cementitious materials, respectively (Nazari and Riahi 2012). The as-received ashes were sieved and the particles passing the finesses of 150 μm and 33 μm were ground using Los Angeles mill for 30 and 180 min, respectively which yielded two different samples for each of FA and RH–BA. The average particle sizes obtained for FA were 75 μm (coarser FA, named cF in this study) and 3 μm (finer FA, named fF in this study) with BET specific surface of 31·3 and 38·9 m^2/g, respectively. The average particle sizes obtained for RH–BA were 90 μm (coarser RH–BA, named cR in this study) and 7 μm (finer RH–BA, named fR in this study) with BET specific surface of 26 and 33·1 m^2/g, respectively. The four produced samples were used in the experiment. Figure 2 shows parti-

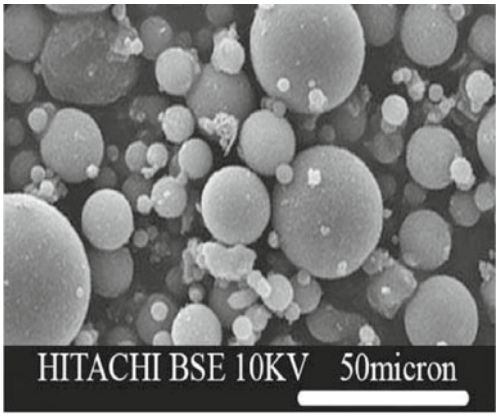

(a)

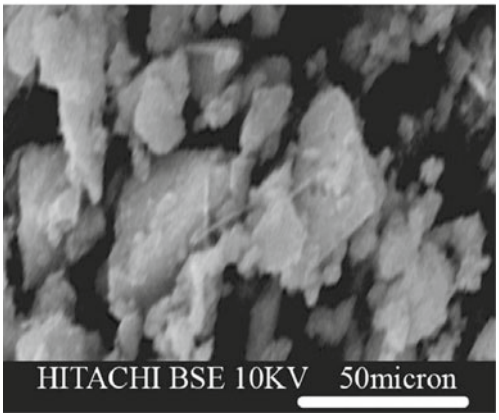

(b)

Figure 1. SEM micrograph of (**a**) FA and (**b**) RH–BA used in this study (Nazari and Riahi 2012).

Table 1. Chemical composition of FA, RH–BA and WG (wt%) (Nazari and Riahi 2012).

Material	SiO_2	Al_2O_3	Fe_2O_3	CaO	SO_3	Na_2O	Loss on ignition
FA	35·21	23·23	12·36	20·01	2·36	0·36	0·24
RH–BA	81·36	0·4	0·12	3·23	0·85	–	3·55
WG	34·21	–	–	–	–	13·11	–

cle size distribution of the four produced samples (Nazari and Riahi 2012).

Sodium silicate solution or water glass (WG) and sodium hydroxide (NaOH) were used as the solution part of the mixture. WG was used without modification, but the sodium hydroxide was diluted to different concentrations before use. The chemical composition of the utilized WG is also given in table 1 (Nazari and Riahi 2012).

Totally 4 series of geopolymer specimens each containing 2 different mixtures of FA and RH–BA as illustrated in table 2 (Nazari and Riahi 2012) were prepared for permeability tests. The mixed alkali activator of sodium silicate solution and sodium hydroxide was used. Sodium hydroxide was diluted by tap water to have concentrations of 4, 8 and 12 M. The solution was left under ambient conditions until excess heat had completely dissipated to avoid accelerating the setting of the geopolymeric specimens. The sodium silicate solution without modification was mixed with sodium hydroxide solution. The ratio of the sodium silicate solution to sodium hydroxide solution was 2·5 by weight for all mixtures because this ratio demonstrated the best properties for fly ash-based geopolymer (Pacheco-Torgal *et al* 2005, 2007). For all samples, the mass ratio of alkali activator to FA–RHA mixture was 0·4. Pastes were mixed by shaking for 5–10 min to give complete homogenization. The mixtures were cast in $\phi 30 \times 60$ mm polypropylene cylinders. The mixing was done in an air-conditioned room at ∼25 °C. The molds were half-filled, vibrated for 45 s, filled to the top, again vibrated for 45 s, and sealed with a lid. The mixtures were then precured for 24 h at room temperature (this precuring time has been found to be beneficial to strength development (Bakharev 2005)). Precuring time before application of heat induces significant dissolution of silica and alumina from fly ash and formation of a continuous matrix phase, increasing, therefore, the homogeneity of the geopolymeric materials (Bakharev 2005; Chindaprasirt *et al* 2007). After the precuring process, samples and molds were placed in a water bath to prevent moisture loss and carbonation of the surface. One batch of these samples was placed in an air-conditioned room at 25 °C. The other batch was put in an oven at elevated temperatures of 50–90 °C for 36 h. To determine the most effective alkali concentration on percentage of water absorption, one set of the specimens cured at 80 °C for 36 h was subjected to permeability tests. Afterwards, the other sets of

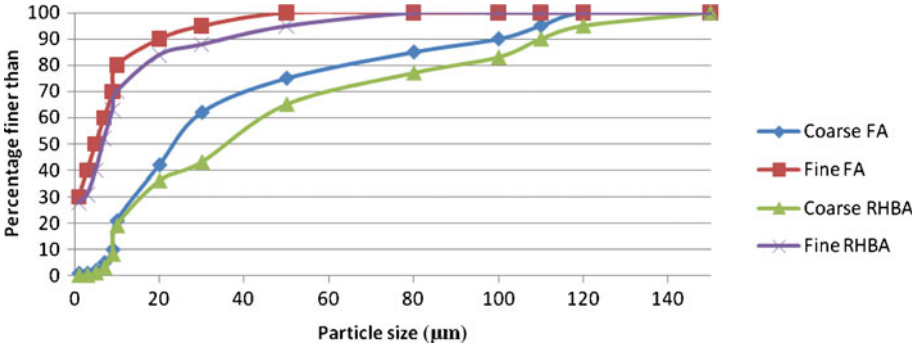

Figure 2. Particle size distribution pattern of different ashes used in this study (Nazari and Riahi 2012).

Table 2. Mixture proportioning of utilized FA and RH–BA to produce geopolymeric specimens (Nazari and Riahi 2012).

Sample designation	Weight percent of fine FA (fF wt%)	Weight percent of coarse FA (cF wt%)	Weight percent of fine RH–BA (fR wt%)	Weight percent of coarse RH–BA (cR wt%)	SiO_2/Al_2O_3 ratio
fF-fR-1	60	0	40	0	3·81
fF-fR-2	70	0	30	0	2·99
fF-fR-3	80	0	20	0	2·38
fF-cR-1	60	0	0	40	3·81
fF-cR-2	70	0	0	30	2·99
fF-cR-3	80	0	0	20	2·38
cF-fR-1	0	60	40	0	3·81
cF-fR-2	0	70	30	0	2·99
cF-fR-3	0	80	20	0	2·38
cF-cR-1	0	60	0	40	3·81
cF-cR-2	0	70	0	30	2·99
cF-cR-3	0	80	0	20	2·38

Alkali activator (WG + NaOH) to FA–RH–BA mixture ratio is 0·4.

Table 3. Percentage of water absorption of geopolymeric specimens (wt%) (Nazari and Riahi 2012).

Age of curing	7 day					28 day				
Temperature of oven curing	25 °C	40 °C	60 °C	80 °C	90 °C	25 °C	40 °C	60 °C	80 °C	90 °C
fF-fR-1	1·61	1·31	1·45	1·06	1·41	1·29	1·05	1·16	0·85	1·13
fF-fR-2	1·26	1·39	1	0·9	1	1·01	1·11	0·8	0·72	0·8
fF-fR-3	1·44	1·49	1·41	1·01	1·13	1·15	1·19	1·13	0·81	0·9
fF-cR-1	1·76	1·49	1·61	1·12	1·49	1·42	1·2	1·3	0·9	1·2
fF-cR-2	1·38	1·51	1·09	0·98	1·09	1·11	1·22	0·88	0·79	0·88
fF-cR-3	1·57	1·62	1·54	1·1	1·23	1·27	1·31	1·24	0·89	0·99
cF-fR-1	2·11	1·78	1·93	1·33	1·78	1·66	1·4	1·52	1·05	1·4
cF-fR-2	1·65	1·82	1·31	1·17	1·31	1·3	1·43	1·03	0·92	1·03
cF-fR-3	1·89	1·94	1·84	1·32	1·47	1·49	1·53	1·45	1·04	1·16
cF-cR-1	2·63	2·22	2·41	1·66	2·22	2·04	1·72	1·87	1·29	1·72
cF-cR-2	2·06	2·27	1·64	1·46	1·64	1·6	1·76	1·27	1·13	1·27
cF-cR-3	2·36	2·43	2·3	1·65	1·84	1·83	1·88	1·78	1·28	1·43

Alkali activator (WG + NaOH) to FA–RH–BA mixture ratio is 0·4.

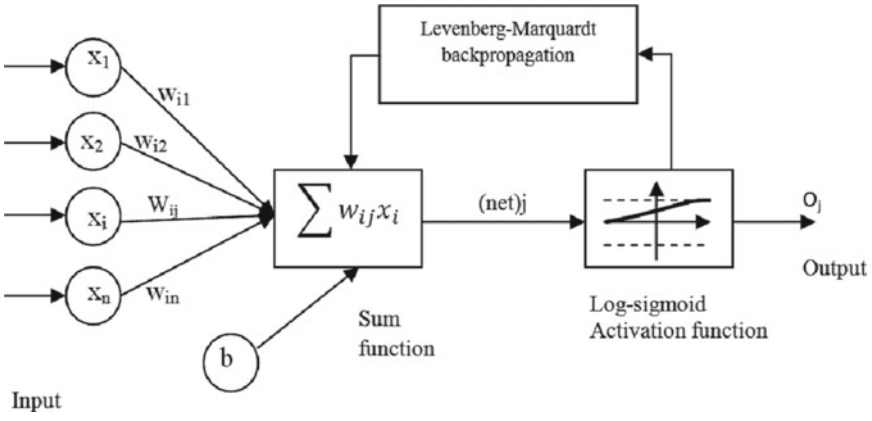

Figure 3. Architecture of applied neural network (Sarıdemir *et al* 2009).

samples were tested at 7 and 28 days of curing (for the specimens cured in elevated temperature, the time of oven-curing were also considered).

To prepare water permeability testing specimens, 1 cm from the top and bottom of the samples from each mixture was removed to avoid any effects caused by surface paste. Hence, the samples having $\phi 30 \times 40$ mm were used as representative specimens for each mixture. Non-shrinking epoxy resin was cast around all specimens with a thickness of 25 mm to prevent water leakage. These specimens were installed in housing cells to test their water permeability. In this work, to evaluate water permeability of the specimens, percentage of water absorption is an evaluation of the pore volume or porosity of concrete after hardening, which is occupied by water in saturated state. Water absorption values of the samples were measured in accordance with the ASTM C 642 after 7 and 28 days of moisture curing adapted to the method done for concrete specimen.

The percentage of water absorption of the produced specimens has been illustrated in table 3 (Nazari and Riahi 2012) for 7 and 28 days of curing. Table 3 (Nazari and Riahi 2012) shows that the best strength has been achieved for fF-fR2 specimen cured at 80 °C for 36 h in both 7 and 28 days curing regimes. As table 3 (Nazari and Riahi 2012) shows, the optimum curing condition for all the mixtures is at 80 °C.

3. Artificial neural networks

ANNs were developed to model the human brain (Topcu *et al* 2008). Even an ANN fairly simple and small in size when compared to the human brain, has some powerful characteristics in knowledge and information processing because of its similarity to the human brain. Therefore, an ANN can be a powerful tool for engineering applications (Ince 2004). McCulloch and Pitts (1943) defined artificial neurons for the first time and developed a neuron model as in figure 3. McCulloch and Pitts (1943) network formed the basis for almost all later neural network models.

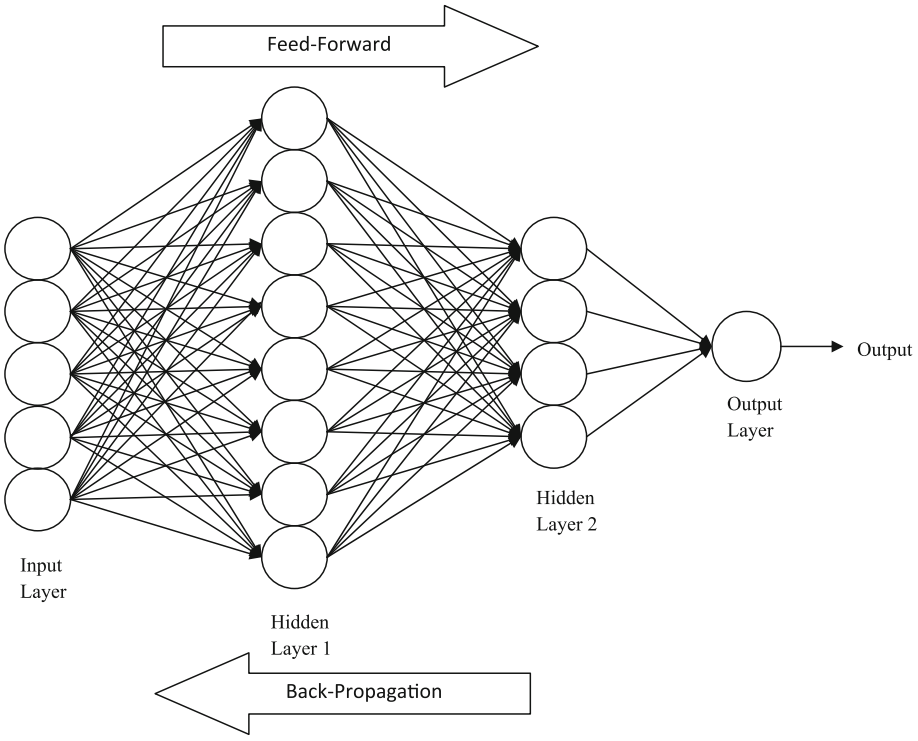

Figure 4. Typical architecture of multilayer perceptron neural network (Sarıdemir *et al* 2009).

1. Initialize the weights and parameter μ (μ = 0.01 is appropriate).
2. Compute the sum of the squared errors over all inputs F(w)

$F(w) = e^T e$

Where $w = [w_1, w_2, \ldots, w_n]$ consists of all weights of the network, e is the error vector comprising the error for all the training examples.

3. Solve (5) to obtain the increment of weights Δw

$\Delta w = [J^T J + \mu I]^{-1} J^T e$

Where J is the Jacobian matrix, μ is the learning rate which is to be updated using the β depending on the outcome. In particular, μ is multiplied by decay rate β ($0<\beta<1$).

4. Using w+Δw as the trial w, and judge
   IF trial F(w)<F(w) in step 2 THEN
   W = w + Δw
   μ = μ.β (β = 0.1)
   go back to step 2
   ELSE
   μ = μ/β
   go back to step 4
   END IF

Figure 5. Pseudo-code for LMBP algorithm (Sarıdemir *et al* 2009).

Afterwards, Rosenblatt (1962) devised a machine called the perceptron that operated much in the same way as the human mind (Sarıdemir *et al* 2009). Saridemir's perceptions consist of "sensory" units connected to a single layer of McCulloch and Pitts (1943) neurons. Rumelhart *et al* (1986) derived a learning algorithm for perceptron networks with constituted hidden units. Their learning algorithm is called back-propagation and is now the most widely used learning algorithm. Figure 4 (Sarıdemir *et al* 2009) shows a typical architecture of a multilayer perceptron neural network with an input layer, two hidden layers and one output layer. As a result of these studies, together with the developments in

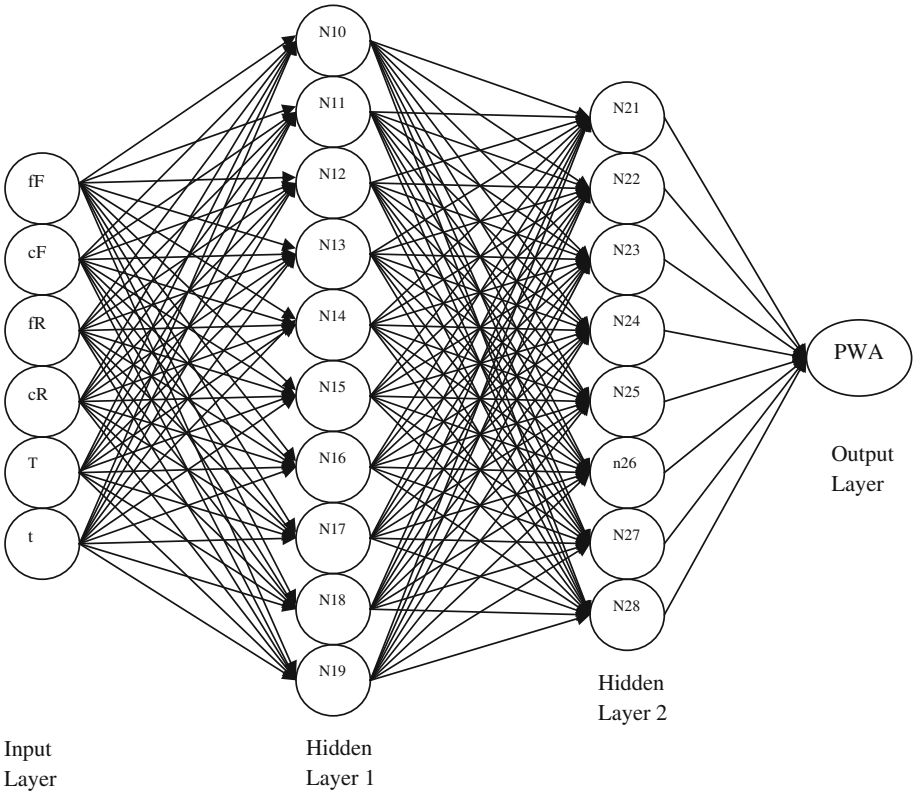

Figure 6. System used in ANN model.

computer technology, using ANN has become more efficient after 1980s (Liu *et al* 2002).

As can be seen from figure 3, an artificial neuron is composed of five main parts: inputs, weights, sum function, activation function and outputs. Inputs are information that enters the neuron from other neurons from external world. Weights are values that express the outcome of an input set or another process element in the preceding layer on this process element. Sum function is a function that calculates the effect of inputs and weights completely on this process element. This function computes the net input that approaches to a neuron (Gunaydın and Dogan 2004). The weighted sums of the input components $(\text{net})_j$ are calculated using (1) as follows:

$$(\text{net})_j = \sum_{i=1}^{n} W_{ij} x_i + b, \tag{1}$$

where $(\text{net})_j$ is the weighted sum of the jth neuron for the input received from the preceding layer with n neurons, W_{ij} the weight between the jth neuron in the previous layer, x_i the output of the ith neuron in the previous layer (Liu *et al* 2002). b is a fix value as internal addition and Σ represents sum function. Activation function is a function that processes the net input obtained from sum function and determines the neuron output. In general, for multilayer feed-forward models as the activation function sigmoid activation function is used. The output of the jth neuron $(\text{out})_j$ is computed using (2) with a sigmoid activation function as follows (Gunaydın and Dogan 2004):

$$O_j = f\,(\text{net})_j = \frac{1}{1 + \sigma^{-\alpha(\text{net})_j}}, \tag{2}$$

where α is a constant used to control the slope of the semi-linear region. The sigmoid nonlinearity activates in every layer except in the input layer. The sigmoid activation function represented by (2) gives outputs in (0, 1). If it is desired, the outputs of this function can be adjusted to $(-1, 1)$ interval. As the sigmoid processor represents a continuous

Table 4. Values of parameters used in neural network model.

Parameters	ANN
Number of input layer units	6
Number of hidden layers	2
Number of first hidden layer units	10
Number of second hidden layer units	8
Number of output layer units	1
Momentum rate	0·88
Learning rate	0·70
Error after learning	0·000050
Learning cycle	30·000

function it is particularly used in nonlinear descriptions. Because its derivatives can be determined easily with regard to the parameters within $(\text{net})_j$ variable (Liu *et al* 2002).

LMBP is often the fastest available back-propagation algorithm, and is highly recommended as a first-choice supervised algorithm, although it requires more memory than other algorithms. The standard LMBP training process can be described in the pseudocode of figure 5 (Suratgar *et al* 2005).

4. Neural network model structure and parameters

ANN model in this research has six neurons in the input layer and one neuron in the output layer as demonstrated in figure 6. The values for input layers were the percentage of fine fly ash in the ashes mixture (fF), the percentage of coarse fly ash in the ashes mixture (cF), the percentage of fine rice husk bark ash in the ashes mixture (fR), the percentage of coarse rice husk bark ash in the ashes mixture (cR), the

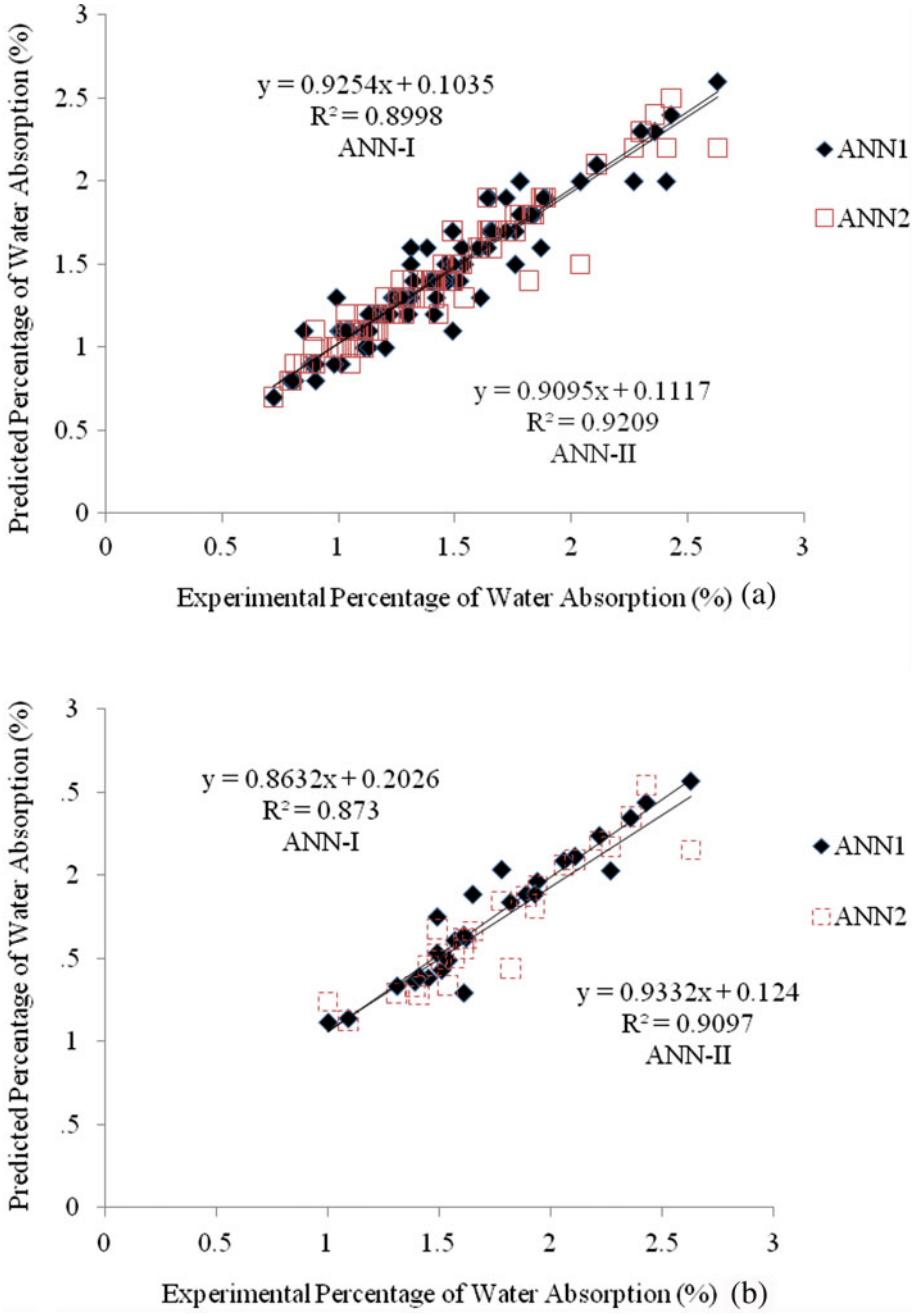

Figure 7. Correlation of measured and predicted percentage of water absorption values of geopolymers in (**a**) training and (**b**) testing phase for ANN models.

Table 5. Data sets for comparison of experimental results with results predicted from ANN models.

Percentage of fine fly ash in ashes mixture (fF)	Percentage of coarse fly ash in ashes mixture (cF)	Percentage of fine rice husk bark ash in ashes mixture (fR)	Percentage of coarse rice husk bark ash in ashes mixture (cR)	Temperature of curing (T)	Time of water curing (t)	Percentage of water absorption values obtained from experiments (%)	Percentage of water absorption values predicted by ANN-I model (%)	Percentage of water absorption values predicted by ANN-II model (%)
60	0	40	0	25	7	1·61	1·3	1·6
70	0	30	0	25	7	1·26	1·3	1·3
80	0	20	0	25	7	1·44	1·4	1·4
60	0	0	40	25	7	1·76	1·7	1·8
70	0	0	30	25	7	1·38	1·6	1·4
80	0	0	20	25	7	1·57	1·6	1·5
0	60	40	0	25	7	2·11	2·1	2·1
0	70	30	0	25	7	1·65	1·9	1·7
0	80	20	0	25	7	1·89	1·9	1·9
0	60	0	40	25	7	2·63	2·6	2·2
0	70	0	30	25	7	2·06	2·1	2·1
0	80	0	20	25	7	2·36	2·3	2·4
60	0	40	0	40	7	1·31	1·3	1·3
70	0	30	0	40	7	1·39	1·4	1·3
80	0	20	0	40	7	1·49	1·5	1·5
60	0	0	40	40	7	1·49	1·7	1·7
70	0	0	30	40	7	1·51	1·4	1·5
80	0	0	20	40	7	1·62	1·6	1·6
0	60	40	0	40	7	1·78	2	1·8
0	70	30	0	40	7	1·82	1·8	1·4
0	80	20	0	40	7	1·94	2	1·9
0	60	0	40	40	7	2·22	2·2	2·2
0	70	0	30	40	7	2·27	2	2·2
0	80	0	20	40	7	2·43	2·4	2·5
60	0	40	0	60	7	1·45	1·4	1·5
70	0	30	0	60	7	1	1·1	1·2
80	0	20	0	60	7	1·41	1·4	1·3
60	0	0	40	60	7	1·61	1·6	1·6
70	0	0	30	60	7	1·09	1·1	1·1
80	0	0	20	60	7	1·54	1·5	1·3
0	60	40	0	60	7	1·93	1·9	1·8
0	70	30	0	60	7	1·31	1·6	1·3
0	80	20	0	60	7	1·84	1·8	1·8
0	60	0	40	60	7	2·41	2	2·2
0	70	0	30	60	7	1·64	1·9	1·9
0	80	0	20	60	7	2·3	2·3	2·3
60	0	40	0	80	7	1·06	1·1	1·3
70	0	30	0	80	7	0·9	0·8	0·9
80	0	20	0	80	7	1·01	0·9	1
60	0	0	40	80	7	1·12	1·1	1·2
70	0	0	30	80	7	0·98	0·9	1
80	0	0	20	80	7	1·1	1·1	1·1
0	60	40	0	80	7	1·33	1·7	1·4
0	70	30	0	80	7	1·17	1·2	1·1
0	80	20	0	80	7	1·32	1·4	1·4
0	60	0	40	80	7	1·66	1·7	1·7
0	70	0	30	80	7	1·46	1·5	1·4
0	80	0	20	80	7	1·65	1·7	1·7
60	0	40	0	90	7	1·41	1·2	1·4
70	0	30	0	90	7	1	1·1	1
80	0	20	0	90	7	1·13	1·2	1·1
60	0	0	40	90	7	1·49	1·1	1·4

Table 5. *(continued).*

Percentage of fine fly ash in ashes mixture (fF)	Percentage of coarse fly ash in ashes mixture (cF)	Percentage of fine rice husk bark ash in ashes mixture (fR)	Percentage of coarse rice husk bark ash in ashes mixture (cR)	Temperature of curing (T)	Time of water curing (t)	Percentage of water absorption values obtained from experiments (%)	Percentage of water absorption values predicted by ANN-I model (%)	Percentage of water absorption values predicted by ANN-II model (%)
70	0	0	30	90	7	1·09	1·1	1·1
80	0	0	20	90	7	1·23	1·3	1·2
0	60	40	0	90	7	1·78	2	1·8
0	70	30	0	90	7	1·31	1·3	1·3
0	80	20	0	90	7	1·47	1·4	1·4
0	60	0	40	90	7	2·22	2·2	2·2
0	70	0	30	90	7	1·64	1·6	1·7
0	80	0	20	90	7	1·84	1·8	1·8
60	0	40	0	25	28	1·29	1·2	1·3
70	0	30	0	25	28	1·01	1·1	1
80	0	20	0	25	28	1·15	1·2	1·1
60	0	0	40	25	28	1·42	1·3	1·4
70	0	0	30	25	28	1·11	1·1	1·2
80	0	0	20	25	28	1·27	1·3	1·3
0	60	40	0	25	28	1·66	1·7	1·6
0	70	30	0	25	28	1·3	1·3	1·3
0	80	20	0	25	28	1·49	1·5	1·5
0	60	0	40	25	28	2·04	2	1·5
0	70	0	30	25	28	1·6	1·6	1·6
0	80	0	20	25	28	1·83	1·8	1·8
60	0	40	0	40	28	1·05	1·1	0·9
70	0	30	0	40	28	1·11	1	1
80	0	20	0	40	28	1·19	1·2	1·2
60	0	0	40	40	28	1·2	1·2	1·3
70	0	0	30	40	28	1·22	1·2	1·2
80	0	0	20	40	28	1·31	1·5	1·3
0	60	40	0	40	28	1·4	1·7	1·5
0	70	30	0	40	28	1·43	1·4	1·2
0	80	20	0	40	28	1·53	1·6	1·5
0	60	0	40	40	28	1·72	1·9	1·7
0	70	0	30	40	28	1·76	1·5	1·7
0	80	0	20	40	28	1·88	1·9	1·9
60	0	40	0	60	28	1·16	1·2	1·1
70	0	30	0	60	28	0·8	0·8	1
80	0	20	0	60	28	1·13	1·2	1·1
60	0	0	40	60	28	1·3	1·2	1·3
70	0	0	30	60	28	0·88	0·9	0·9
80	0	0	20	60	28	1·24	1·3	1·2
0	60	40	0	60	28	1·52	1·4	1·5
0	70	30	0	60	28	1·03	1·1	1·2
0	80	20	0	60	28	1·45	1·4	1·5
0	60	0	40	60	28	1·87	1·6	1·9
0	70	0	30	60	28	1·27	1·3	1·6
0	80	0	20	60	28	1·78	1·8	1·8
60	0	40	0	80	28	0·85	1·1	0·9
70	0	30	0	80	28	0·72	0·7	0·7
80	0	20	0	80	28	0·81	0·8	0·9
60	0	0	40	80	28	0.9	0·9	1·1
70	0	0	30	80	28	0·79	0·8	0·8
80	0	0	20	80	28	0·89	0·9	1
0	60	40	0	80	28	1·05	1·1	1·1
0	70	30	0	80	28	0·92	0·9	0·9

Table 5. *(continued).*

Percentage of fine fly ash in ashes mixture (fF)	Percentage of coarse fly ash in ashes mixture (cF)	Percentage of fine rice husk bark ash in ashes mixture (fR)	Percentage of coarse rice husk bark ash in ashes mixture (cR)	Temperature of curing (T)	Time of water curing (t)	Percentage of water absorption values obtained from experiments (%)	Percentage of water absorption values predicted by ANN-I model (%)	Percentage of water absorption values predicted by ANN-II model (%)
0	80	20	0	80	28	1·04	1·1	1
0	60	0	40	80	28	1·29	1·3	1·3
0	70	0	30	80	28	1·13	1·1	1·1
0	80	0	20	80	28	1·28	1·3	1·2
60	0	40	0	90	28	1·13	1	1·1
70	0	30	0	90	28	0·8	0·8	0·8
80	0	20	0	90	28	0·9	0·9	0·9
60	0	0	40	90	28	1·2	1	1·2
70	0	0	30	90	28	0·88	1·1	0·9
80	0	0	20	90	28	0·99	1·3	1
0	60	40	0	90	28	1·4	1·4	1·4
0	70	30	0	90	28	1·03	1·1	1·1
0	80	20	0	90	28	1·16	1·2	1
0	60	0	40	90	28	1·72	1·7	1·7
0	70	0	30	90	28	1·27	1·3	1·4
0	80	0	20	90	28	1·43	1·4	1·2

temperature of curing (T) and the time of water curing (t). The value for output layer was percentage of water absorption (PWA). Two hidden layers with ten and eight neurons were used in the architecture of multilayer neural network because of its minimum absolute percentage error values for training and testing sets. The neurons of neighbouring layers are completely interconnected by weights. Finally, the output layer neurons produce the network prediction as a result.

In this study, the back-propagation training algorithm has been utilized in feed-forward two hidden layers. Back-propagation algorithm, as one of the most well known training algorithms for the multilayer perceptron, is a gradient descent technique to minimize the error for a particular training pattern in which it adjusted the weights by a small amount at a time (Suratgar *et al* 2005). The nonlinear sigmoid activation function was used in the hidden layer and the neuron outputs at the output layer. Momentum rate and learning rate values were determined and the model was trained through iterations. The trained model was only tested with the input values and the predicted results were close to experimental results. The values of parameters used in neural network model are given in table 4.

Totally 120 data of permeability tests in different conditions were collected, trained and tested by means of ANNs. Among 120 experimental sets, 94 sets were randomly chosen as a training set for the ANN-I and ANN-II modelling and the remaining 26 sets were used as testing the generalization capacity of the proposed models.

To make a decision on the completion of the training processes, two termination states are declared: state 1 (ANN-I model) means that the training of neural network ended when the maximum epoch of process reached (1000) while state 2 (ANN-II model) means the training ended when minimum error norm of network gained.

The performance of a ANN model mainly depends on the network architecture and parameter settings. One of the most difficult tasks in ANN studies is to find this optimal network architecture, which is based on the determination of numbers of optimal layers and neurons in the hidden layers by a trial and error approach. The assignment of initial weights and other related parameters may also influence the performance of ANN to a great extent. However, there is no well defined rule or procedure to have an optimal network architecture and parameter settings where the trial and error method still remains valid. This process is very time consuming (Guzelbey *et al* 2006).

In this study, the Matlab ANN toolbox is used for ANN applications. To overcome optimization difficulty, a program has been developed in Matlab which handles the trial and error process automatically (Guzelbey *et al* 2006). The program tries various number of layers and neurons in the hidden layers both for the first and second hidden layers when the highest root mean squared error (RMSE) of the testing set, as the training of the testing set is achieved (Guzelbey *et al* 2006).

5. Results and discussion

In this study, the error arose during the training and testing of ANN-I and ANN-II models and can be expressed as absolute

fraction of variance (R^2) which are calculated by (3) (Topcu and Sarıdemir 2008):

$$R^2 = 1 - \left(\frac{\sum_i (t_i - o_i)^2}{\sum_i (o_i)^2} \right), \tag{3}$$

where t is the target value and o the output value.

All of the results obtained from experimental studies and predicted by using the training and testing results of ANN-I and ANN-II models are given in figures 7a and b, respectively. The linear least square fit line, its equation and the R^2 values were shown in these figures for the training and testing data. Also, input values and experimental results with training and testing results obtained from ANN-I and ANN-II models are given in table 5. As it is visible in figure 7, values obtained from the training and testing in ANN-I and ANN-II models are very close to the experimental results. The result of testing phase in figure 7 shows that the ANN-I and ANN-II models are capable of generalizing between input and output variables with reasonably good predictions.

The performance of ANN-I and ANN-II models are shown in figure 7. The best value of R^2 is 99·90 % for training set in the ANN-II model. The minimum values of R^2 is 95·74 % for testing set in ANN-I model. All of R^2 values show that the proposed ANN-I and ANN-II models are suitable and can predict the permeability values very close to the experimental values.

6. Conclusions

From the experimental procedure, the following results were obtained:

(I) ANNs can be used an alternative approach for the evaluation of the effect of seeded mixture of FA and RH–BA on percentage of water absorption values of geopolymer specimens.

(II) Comparison between ANNs in terms of R^2 showed that ANNs models are capable to predict suitable results for percentage of water absorption values of geopolymer specimens.

References

Álvarez-Ayuso E *et al* 2008 *J. Hazard. Mater.* **154** 175

Bakharev T 2005 *Cement Concr. Res.* **35** 1224

Barbosa V F F, MacKenzie K J D and Thaurmaturgo C 2000 *Int. J. Inorg. Mater.* **2** 309

Chindaprasirt P, Chareerat T and Sirivivatnanon V 2007 *Cement Concr. Compos.* **29** 224

Cottrell G A, Kemp R, Bhadeshia H K D H, Odette G R and Yamamoto T 2007 *J. Nucl. Mater.* **367** 603

Davidovits J 2008 *Geopolymer chemistry and applications* (St. Quentin: Geopolymere Institut)

Fanhong K and Maoyu Z 2008 *Energy Build* **40** 1614

Gunaydın H M and Dogan S Z 2004 *Int. J. Project Manage.* **22** 595

Guzelbey I H, Cevik A and Erklig A 2006 *J. Constr. Steel Res.* **62** 962

Ince R 2004 *Eng. Fract. Mech.* **71** 2143

Liu S W, Huang J H, Sung J C and Lee C C 2002 *Comput. Meth. Appl. Mech. Eng.* **191** 2831

McCulloch W S and Pitts W 1943 *Bull. Math. Biophys.* **5** 115

Nazari A and Riahi S 2012 *J. Non-Cryst. Solids* **358** 40

Pacheco-Torgal F, Castro-Gomes J P and Jalali S 2005 *Studies about mix composition of alkali-activated, mortars using waste mud from Panasqueira*. in *Proceedings of the engineering conference* (Covilha, Portugal: University of Beira Interior)

Pacheco-Torgal F, Castro-Gomes J and Jalali S 2007 *Cem. Concr. Res.* **37** 933

Pak J, Jang J, Bhadeshia H K D H and Karlsson L 2009 *Mater. Manuf. Process.* **24** 16

Pala M, Ozbay O, Oztas A and Yuce M I 2005 *Constr. Build. Mater.* **21** 384

Rosenblatt F 1962 *Principles of neuro dynamics: perceptrons and the theory of brain mechanisms* (Washington DC: Spartan Books)

Rumelhart D E, Hinton G E and William R J 1986 *Learning internal representation by error propagation*, in *Proceeding parallel distributed processing foundation* (eds) D E Rumelhart and J L McClelland (Cambridge: MIT Press)

Sarıdemir M, Topcu I B, Ozcan F and Severcan M H 2009 *Constr. Build. Mater.* **23** 1279

Sata V, Jaturapitakkul C and Kiattikomol K 2007 *Constr. Build Mater.* **21** 1589

Suratgar A A, Tavakoli M B and Hoseinabadi A 2005 *World Acad. Sci. Eng. Technol.* **6** 46

Tariku F, Kumaran K and Fazio P 2010 *Int. J. Heat Mass Tran.* **53** 3035

Topcu I B and Sarıdemir M 2008 *Comp. Mater. Sci.* **41** 305

Topcu I B, Karakurt C and Sarıdemir M 2008 *Mater. Design* **29** 1986

van Jaarsveld J G S, van Deventer J S J and Lorenzen L 1997 *Miner. Eng.* **10** 659

Wongpa J, Kiattikomol K, Jaturapitakkul C and Chindaprasirt P 2010 *Mater. Design* **31** 4748